CP violating top-Higgs coupling at future muon collider

HIGGS 2024
Uppsala, Sweden

Ya-Juan Zheng
（Iwate University, Japan）

November 5, 2024

Based on [1] Vernon Barger, Kaoru Hagiwara and YJZ, Phys.Lett.B 850 (2024) 138547.
     [2] Morgan Cassidy, Zhongtian Dong, Kyoungchul Kong, Ian Lewis, Yanzhe Zhang and YJZ, JHEP05(2024) 176.
     [3] Kaoru Hagiwara, Junichi Kanzaki, Olivier Mattelaer, Kentarou Mawatari and YJZ, Phys.ReV.D 110 (2024) 5, 056024.

Outline

- CP violating top Yukawa from effective Lagrangian

- LHC searches and e^-e^+ collider prospect ⟶ muon collider process

- Gauge invariant Lagrangian from a dimension-6 operator

- Unitarity constraints

- Individual diagram contributions in the Feynman-Diagram gauge

LHC searches and constraints

$$\mathcal{L}_{ttH} = -gH\bar{t}(\cos\xi + i\gamma_5 \sin\xi)t$$

g is real and positive, $-\pi < \xi < \pi$

When $g = g_{SM} = m_t/v$, $\xi = 0$ $\longrightarrow$ SM

- X. Zhang, S. K. Lee, K. Whisnant, and B. L. Young, "Phenomenology of a nonstandard top quark Yukawa coupling," Phys. Rev. D 50 (1994) 7042–7047, arXiv:hep-ph/9407259.

- H. Bahl, E. Fuchs, S. Heinemeyer, J. Katzy, M. Menen, K. Peters, M. Saimpert, and G. Weiglein, "Constraining the CP structure of Higgs-fermion couplings with a global LHC fit, the electron EDM and baryogenesis," Eur. Phys. J. C 82 (2022) no. 7, 604, arXiv:2202.11753 [hep-ph].

- ...
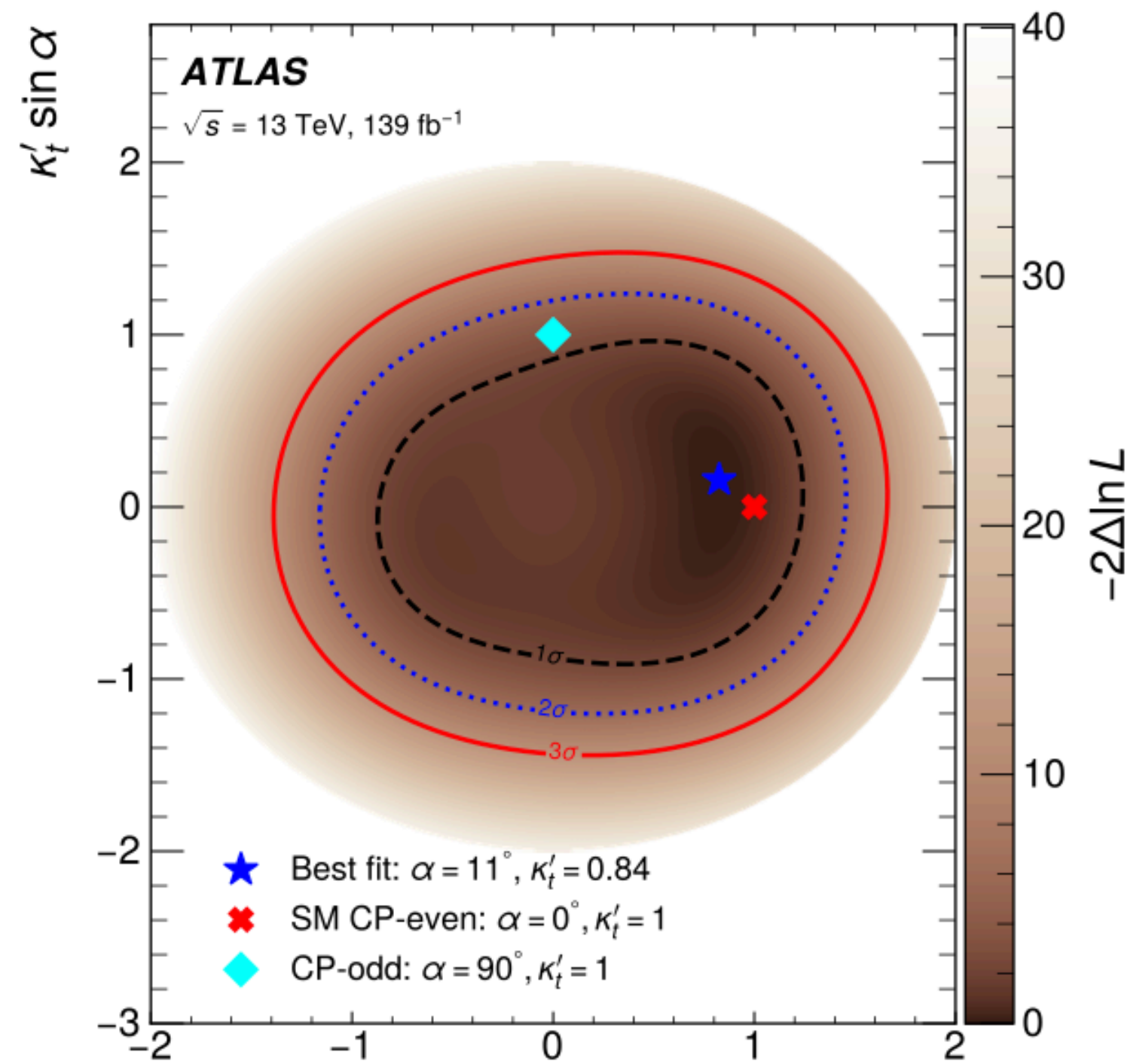
ATLAS: ttH+tH, H>bb
arXiv:2303.05974
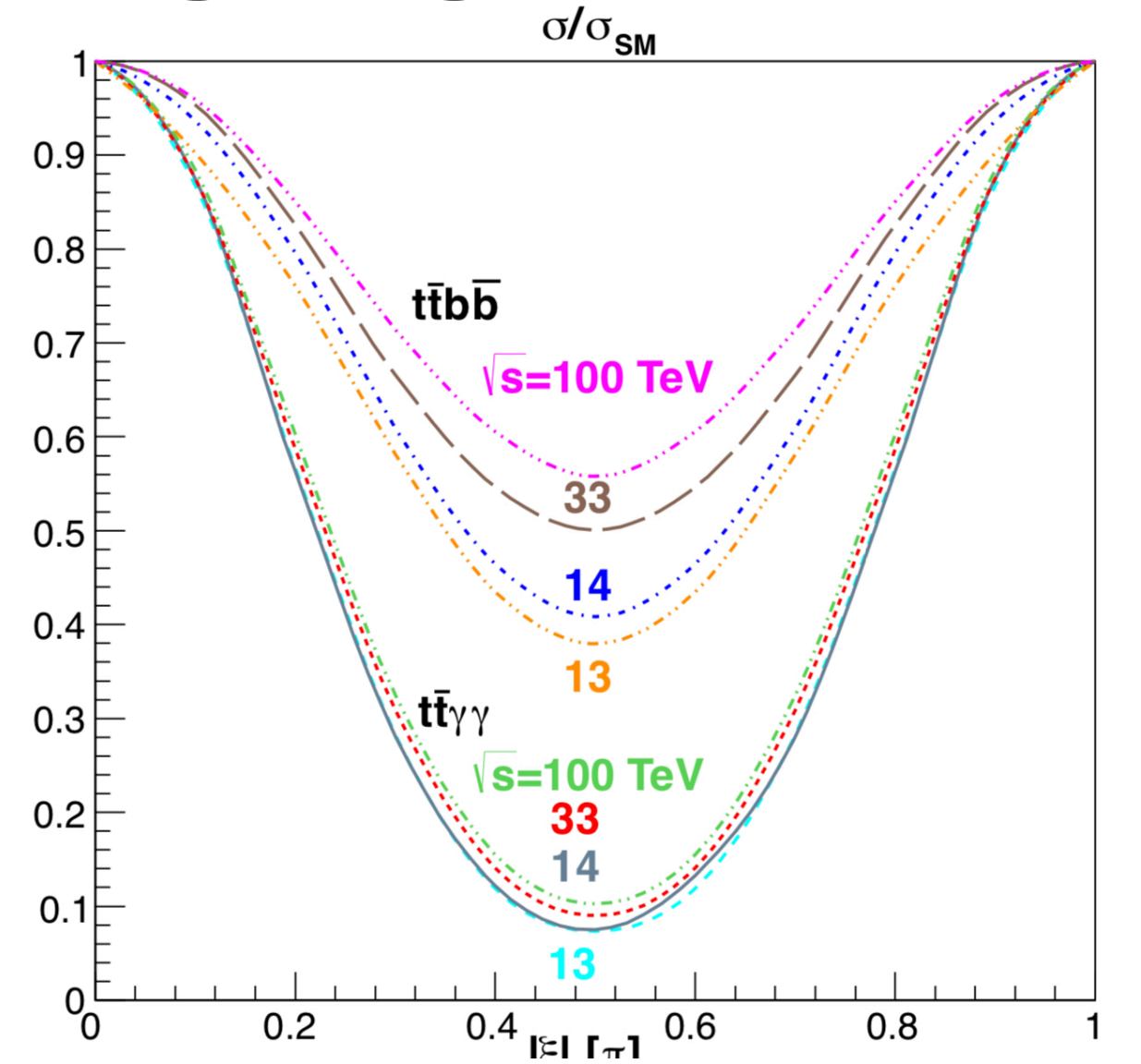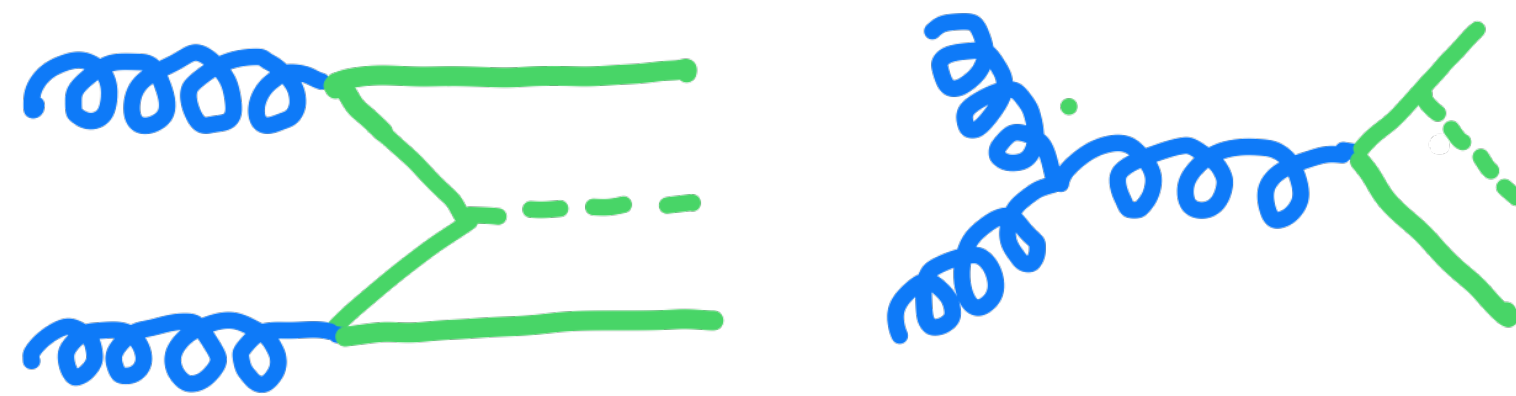
LHC direct searches:
ATLAS best fit: 11+52-73 degree
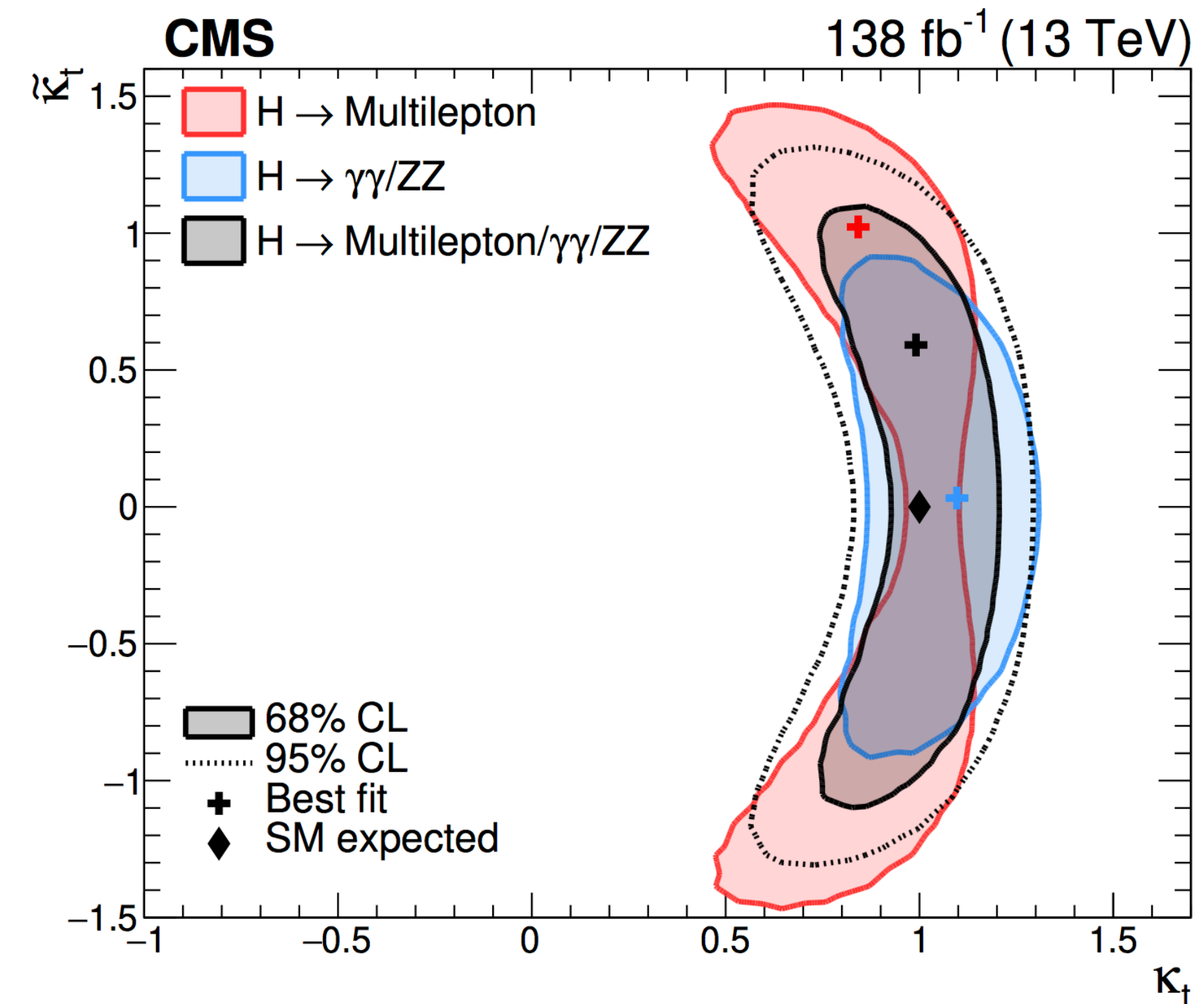
CMS: ttH+tH, H>ls/rr/ZZ
JHEP07(2023)092

Direct measurement of a CP violating top-Higgs Yukawa Lagrangian at LHC and e^-e^+ collider

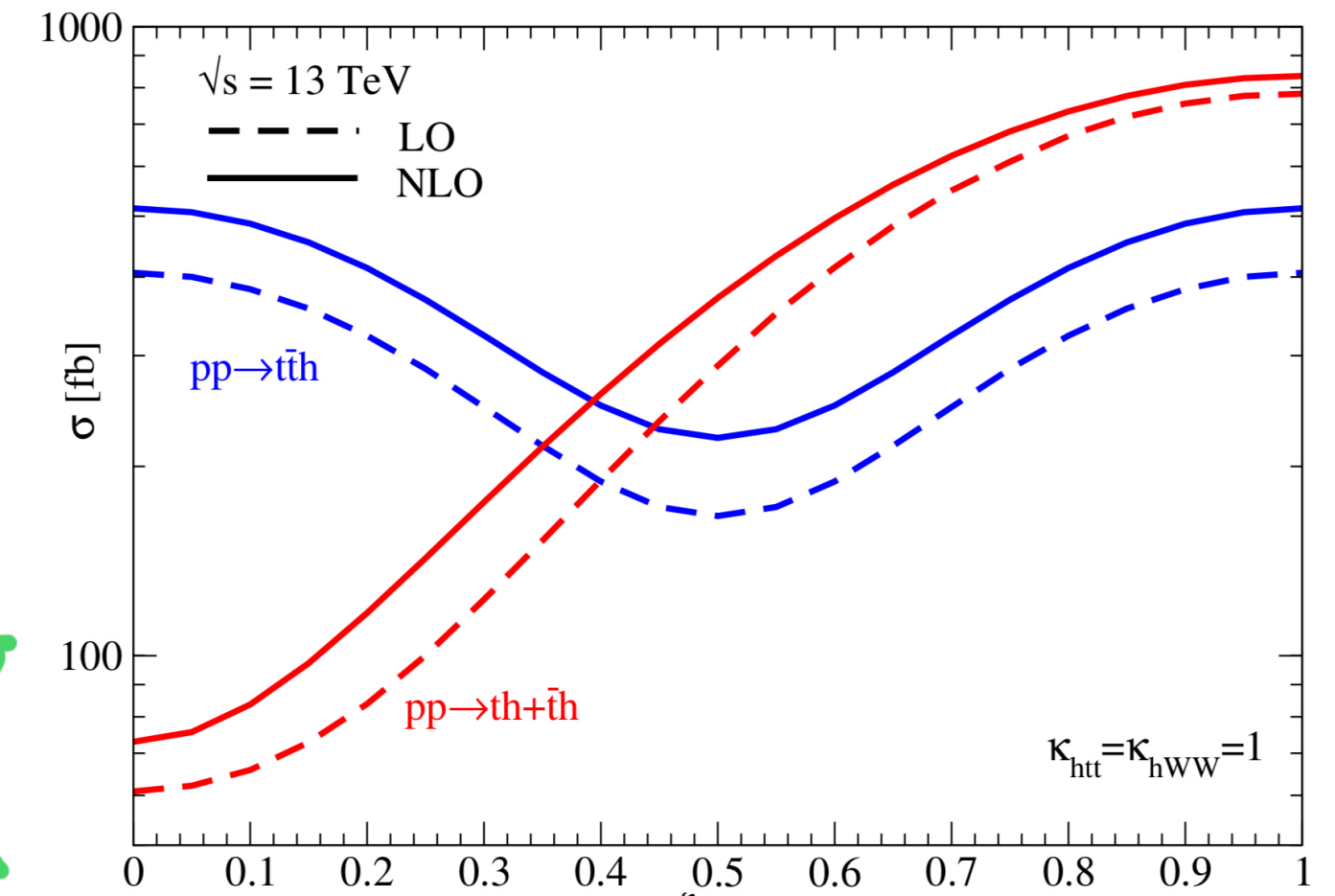$$\mathcal{L}_{ttH} = -gH\bar{t}(\cos\xi + i\gamma_5 \sin\xi)t$$

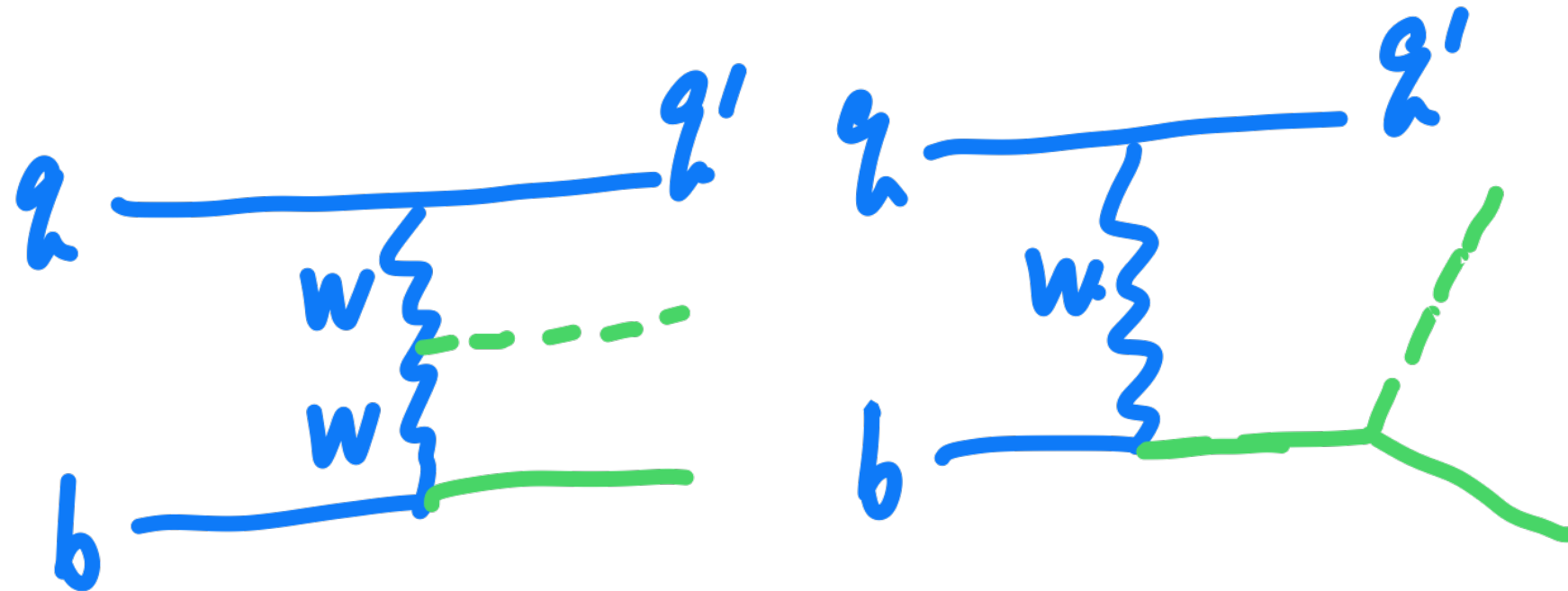**Top pair + Higgs**, $pp \to ttH$

X.G.He, G.N.Li, YJZ. *Int.J.Mod.Phys.A30(2015) 25,1550156.*

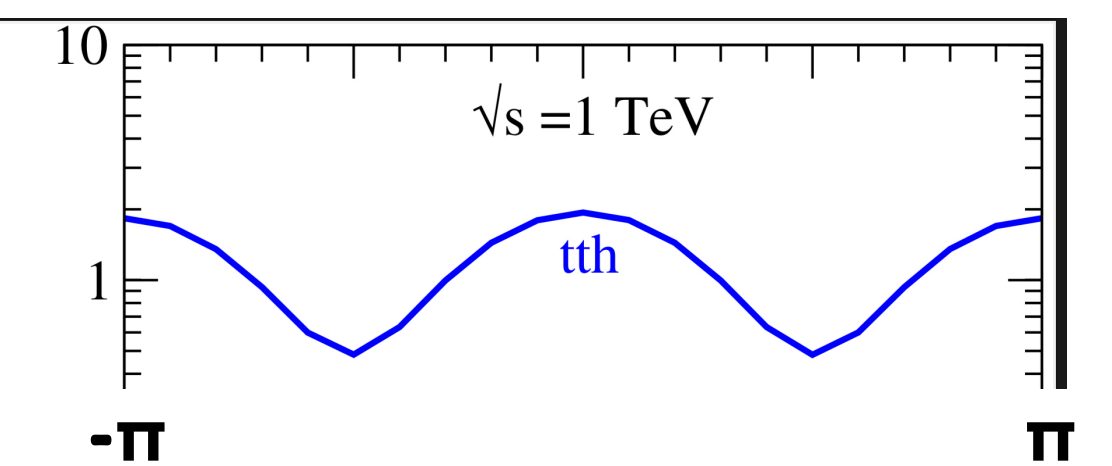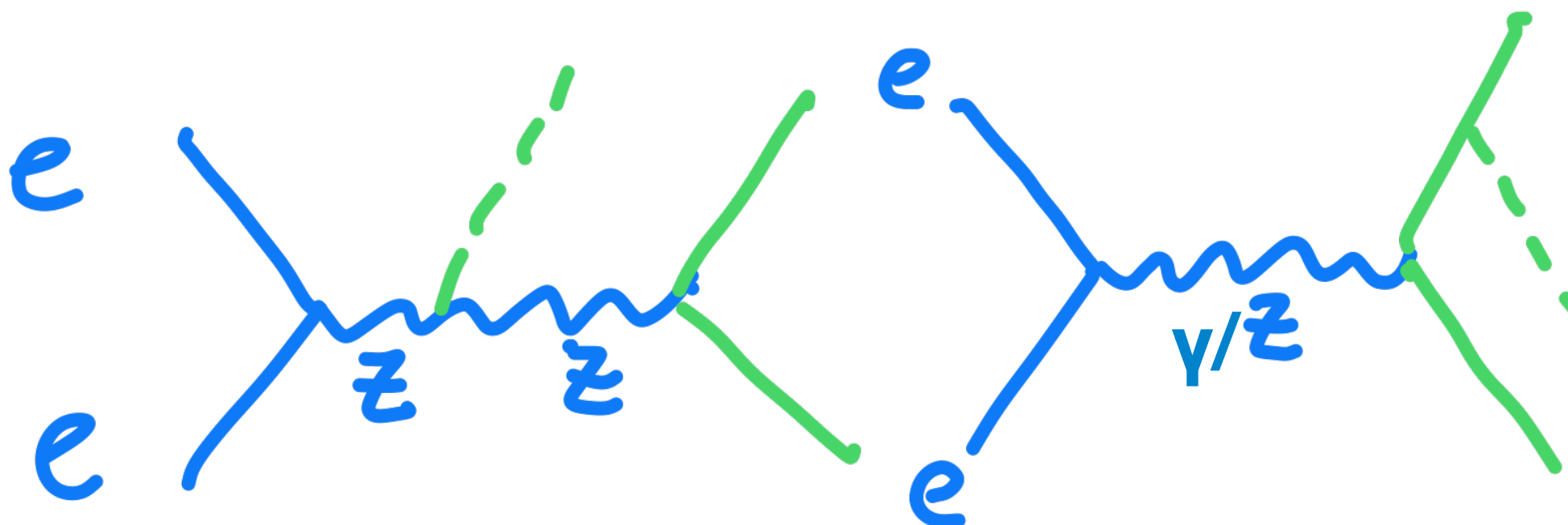**Single top + Higgs**, $pp \to tHj$

V.Barger, K. Hagiwara, YJZ.
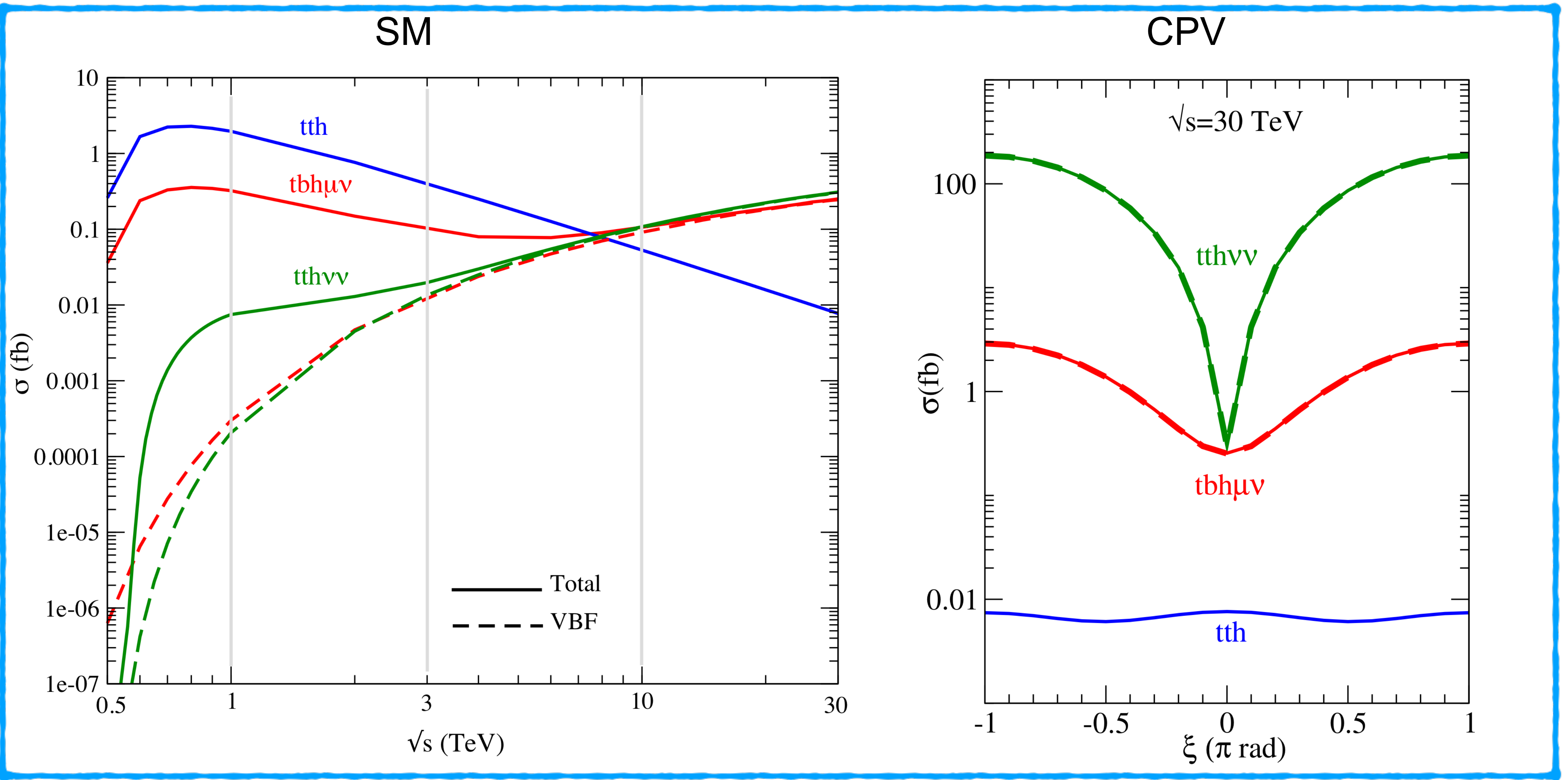*Phys.Rev.D99(2019)3,031701, JHEP09(2020)101.*

Top pair + Higgs, ee →ttH

K. Hagiwara, H.Yokoya, YJZ. JHEP02(2018)180

Top Yukawa processes at muon collider

M.Cassidy, Z.Dong, KC.Kong, I. Lewis, Y.Zhang and YJZ, JHEP 05 (2024) 176.

$\nu_\mu \bar{\nu}_\mu t\bar{t}H$ at future muon collider

$\sigma(\mu^- \mu^+ \rightarrow \nu_\mu \bar{\nu}_\mu t\bar{t}H)$ (fb)

$\sqrt{s} = 100\text{TeV}$
$\sqrt{s} = 30\text{TeV}$
$\sqrt{s} = 10\text{TeV}$
$\sqrt{s} = 3\text{TeV}$
$\sqrt{s} = 1\text{TeV}$

$\sigma(\mu^- \mu^+ \rightarrow \nu_\mu \bar{\nu}_\mu t\bar{t}H)$ (fb)

$\xi = \pi$
$\xi = 0.5\pi$
$\xi = 0.25\pi$
$\xi = 0.1\pi$
$\xi = 0(\text{SM})$
$(\sqrt{s})^2/(100\text{TeV})^2 * \sigma_{100\text{TeV}}^{\xi}$
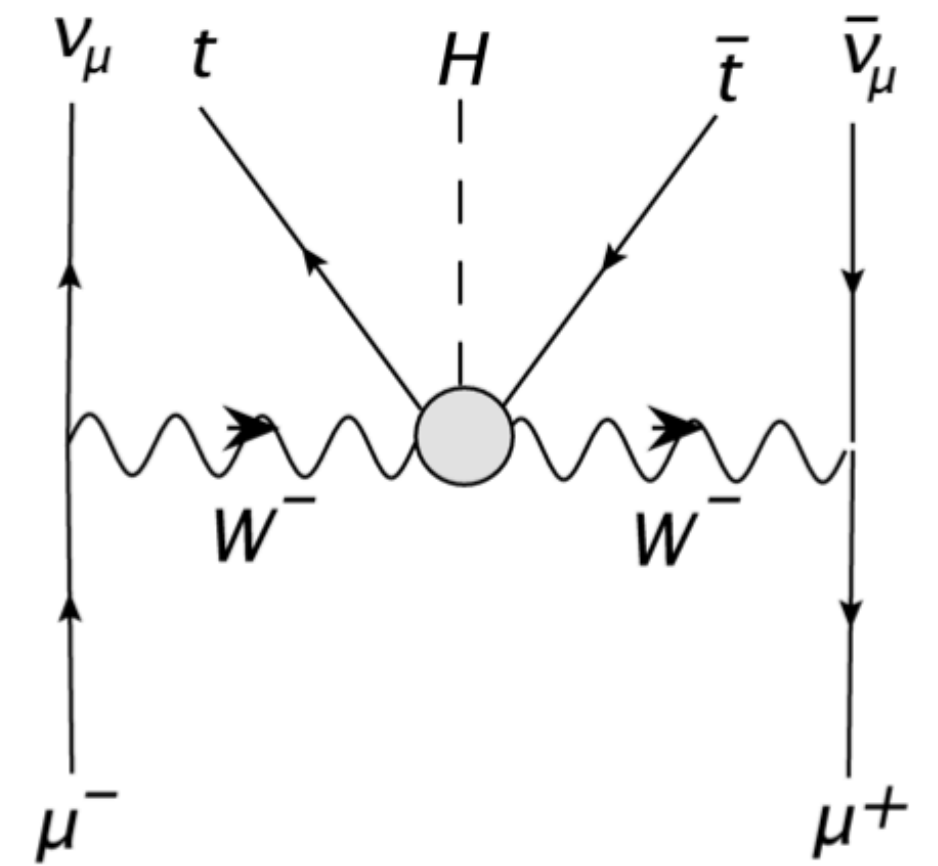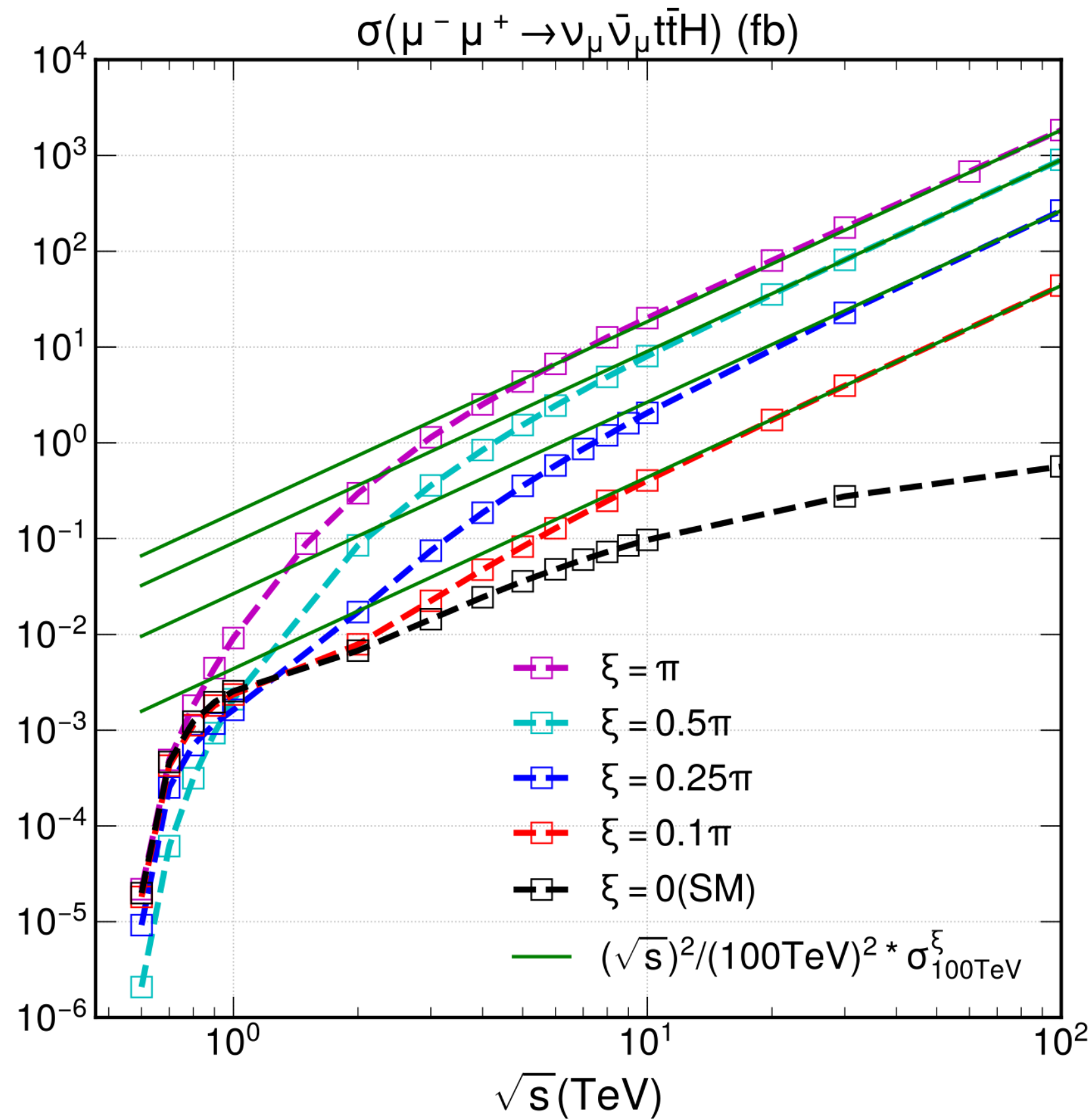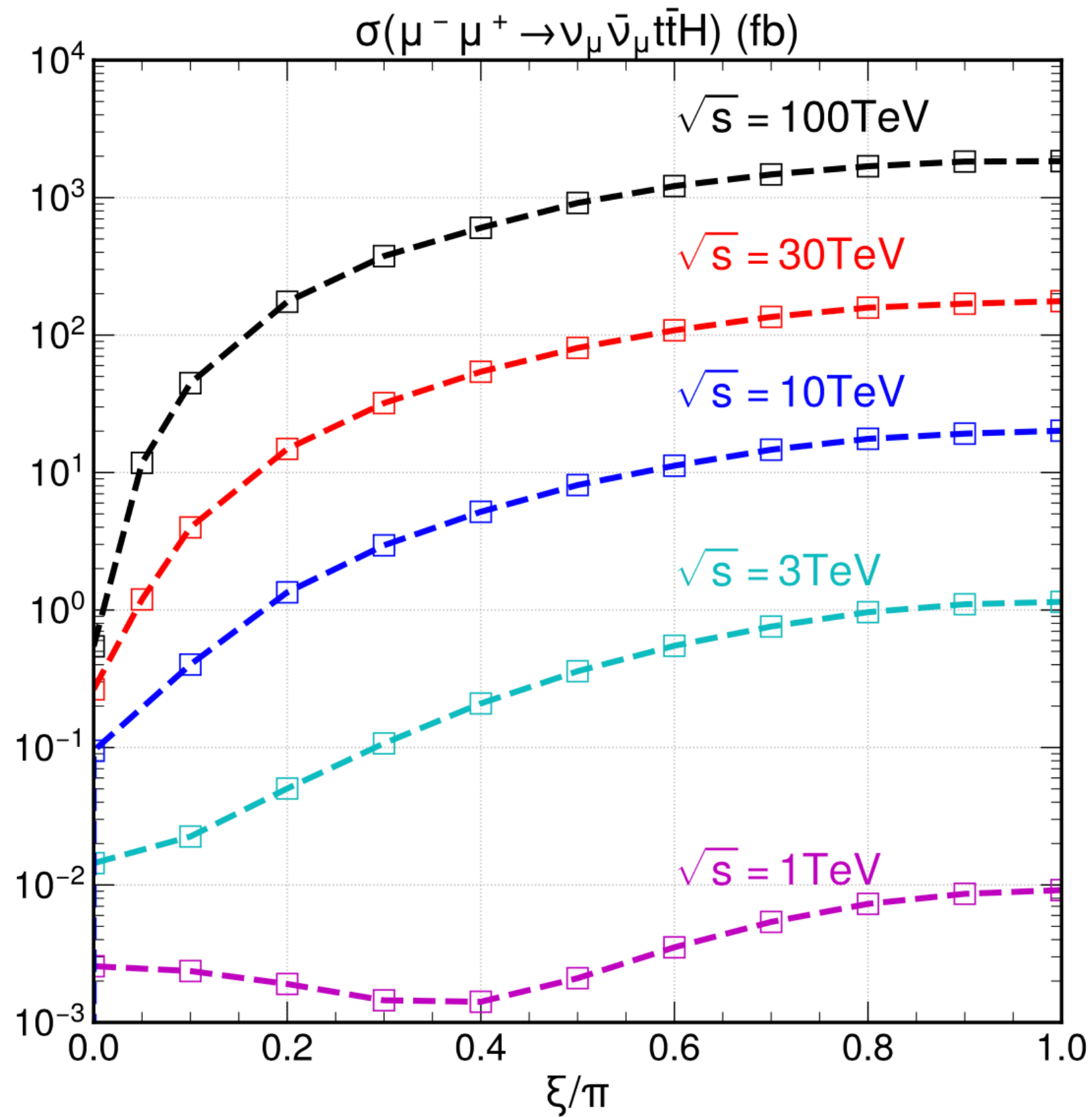
88 diagrams generated from Madgraph5, 20 diagrams are Vector Boson Fusions

Vector Boson Fusion

ξ dependence:
at low energy: s-channel diagrams contribute.
at high energy: t-channel (VBF) dominates.

Energy dependence at high energy:
BSM: quadratic growth
SM: logarithmically growth

Dominate sub-diagrams $W_L^- W_L^+ \to t\bar{t}H$

$\sigma(W_L^- W_L^+ \to t\bar{t}H)$ (fb)

Legend:
- Complex Yukawa
- $(\sqrt{\hat{s}})^2/(100\text{TeV})^2 * \sigma_{100\text{TeV}}^{\xi}$
- $\xi = \pi$
- $\xi = 0.5\pi$
- $\xi = 0.25\pi$
- $\xi = 0.1\pi$

$\xi = 0(\text{SM})$

$\sqrt{\hat{s}}$ (TeV)
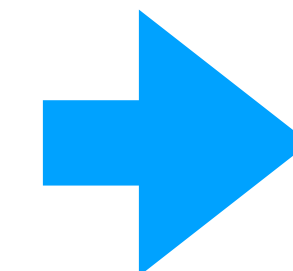
$$W^-(q, h=0)\, W^+(\bar{q}, \bar{h}=0) \to t\bar{t}H$$
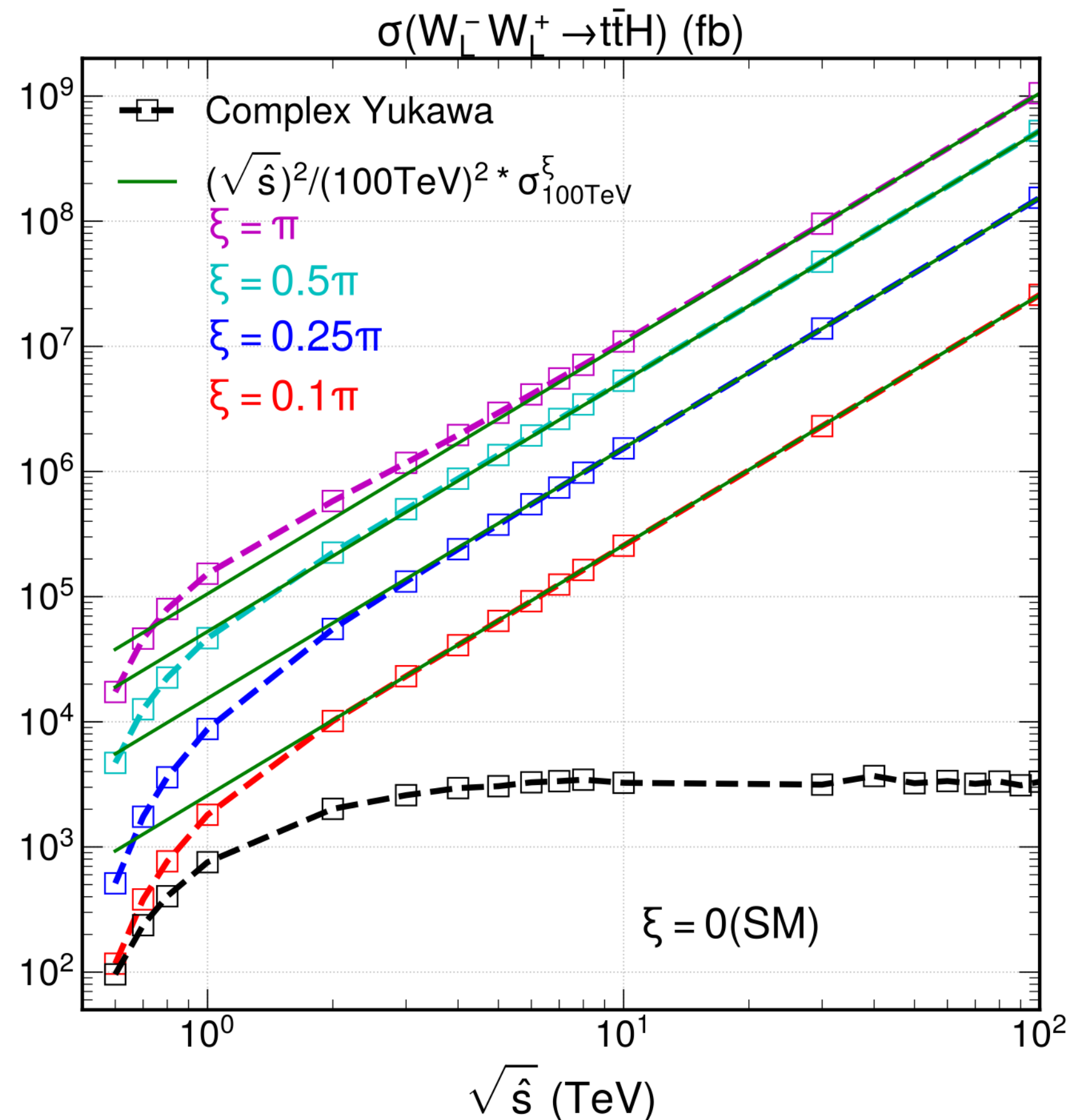
$\xi \neq 0$ **quadratic energy growth** from the longitudinally polarized weak boson wave functions **E/m$_W$**.

$\xi = 0$ In the SM, **E/m$_W$** from individual diagram **cancels** after summing up, leading to the **Goldstone boson equivalence theorem** (GBET) as a manifestation of gauge invariance.
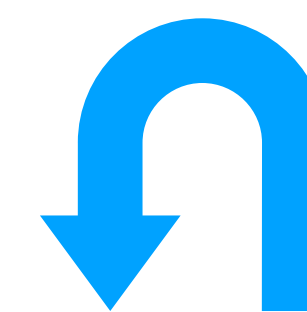
$$\mathcal{L}_{ttH} = -gH\bar{t}(\cos\xi + i\gamma_5 \sin\xi)t$$

Gauge invariant formulation: Models like two Higgs doublet models, etc

Energy dependence at high energy:
BSM: quadratic growth from (**E/m$_W$**)^2, with E=$\sqrt{\hat{s}}/2$
SM: constant

SMEFT

A gauge invariant top Yukawa sector

Dimension-6 operator

$$\mathcal{L} = -y_{\text{SM}} \boxed{Q^\dagger \phi t_R} + \frac{\lambda}{\Lambda^2} \boxed{Q^\dagger \phi t_R} \left(\boxed{\phi^\dagger \phi} - \frac{v^2}{2} \right) + \text{h.c.}$$
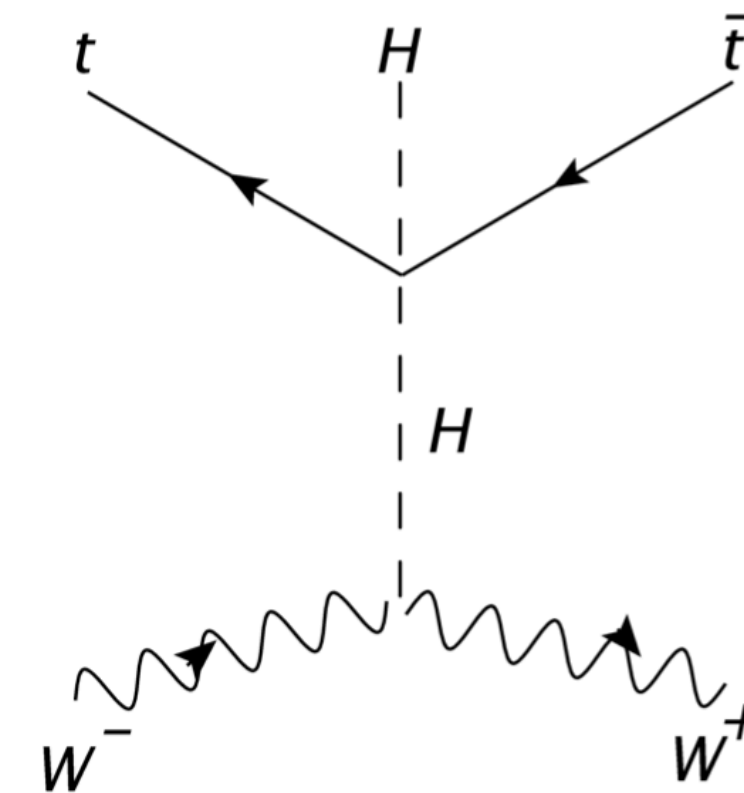
$$Q = (t_L, b_L)^T$$
$$\phi = ((v + H + i\pi^0)/\sqrt{2}, i\pi^-)^T$$

$$
\begin{aligned}
\mathcal{L}_{ttH}^{\text{SMEFT}} =& -m_t t_L^\dagger t_R - g_{\text{SM}} \left[(H + i\pi^0)t_L^\dagger + i\sqrt{2}\pi^- b_L^\dagger \right] t_R \\
& -(ge^{i\xi} - g_{\text{SM}}) \left\{ H t_L^\dagger t_R + \frac{H}{v} \left[(H + i\pi^0)t_L^\dagger + i\sqrt{2}\pi^- b_L^\dagger \right] t_R \right\} \\
& -(ge^{i\xi} - g_{\text{SM}}) \left\{ \left[\frac{H^2 + (\pi^0)^2}{2v} + \frac{\pi^+\pi^-}{v} \right] t_L^\dagger t_R \right. \\
& \left. + \frac{H^2 + (\pi^0)^2 + 2\pi^+\pi^-}{2v^2} \left[(H + i\pi^0)t_L^\dagger + i\sqrt{2}\pi^- b_L^\dagger \right] t_R \right\} + \text{h.c.},
\end{aligned}
$$

$$\boxed{g_{\text{SM}} = \frac{y_{\text{SM}}}{\sqrt{2}} = \frac{m_t}{v}}$$ $$\boxed{\frac{g_{\text{SM}} - ge^{i\xi}}{v^2} = \frac{\lambda}{\Lambda^2}}$$
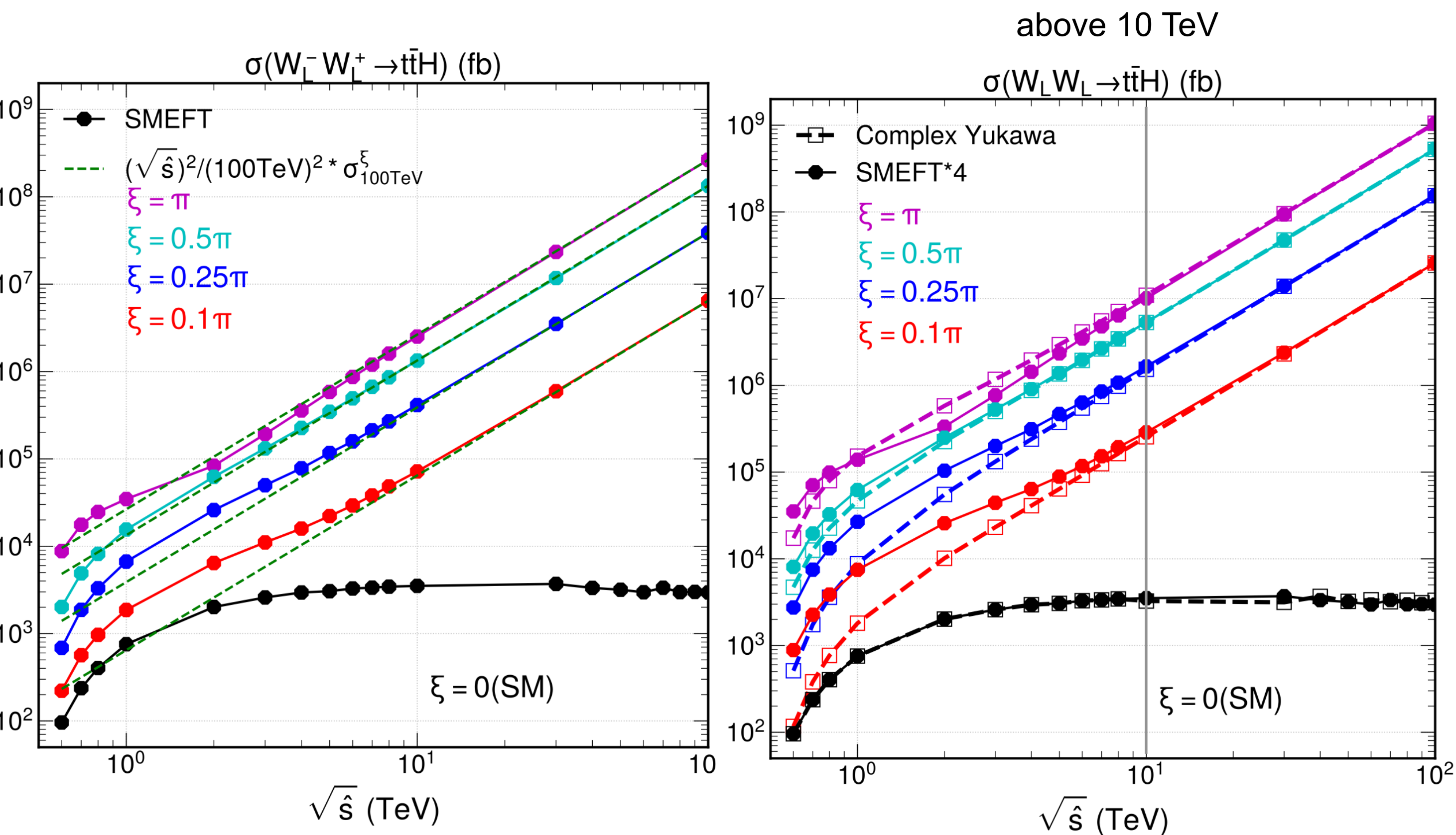
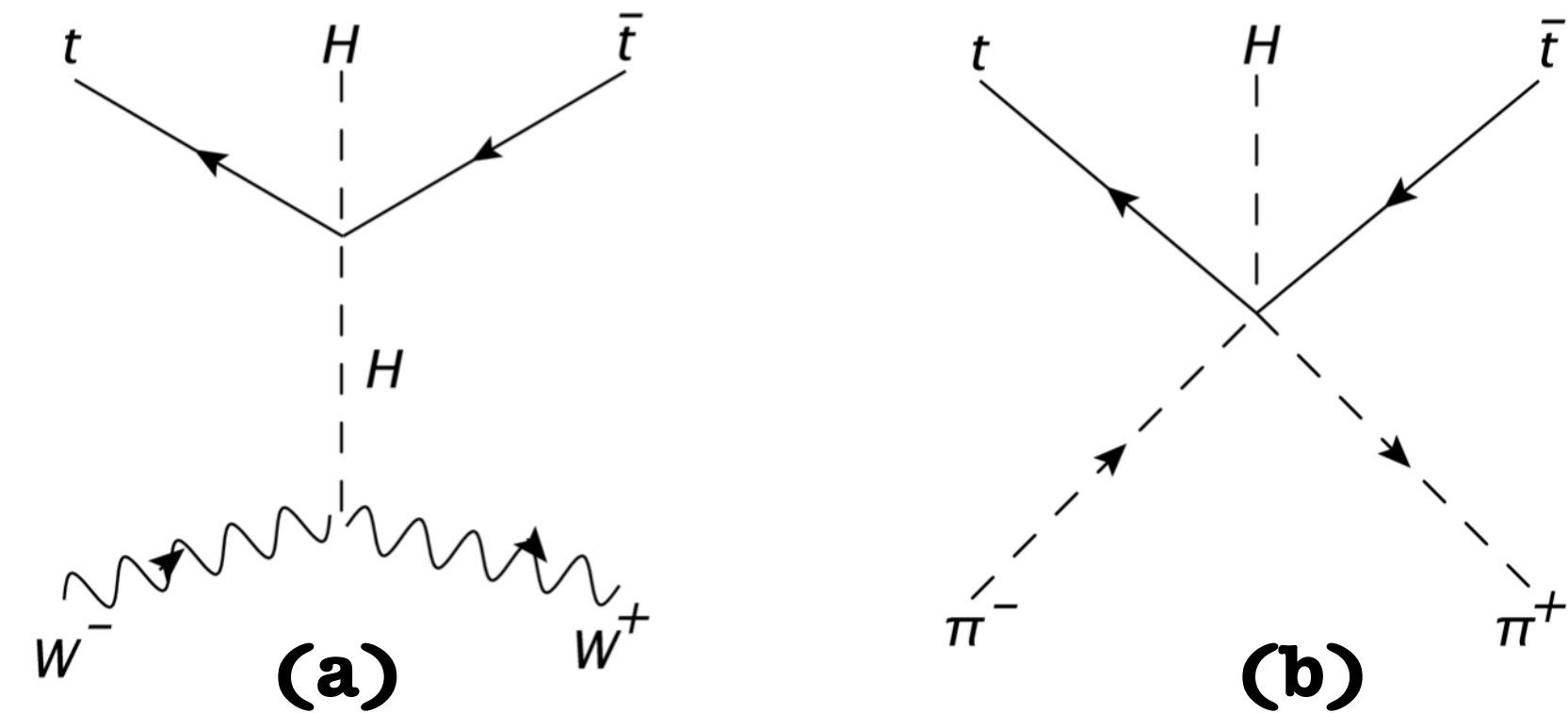Additional ttHH and ttHHH coupling

$$\boxed{\mathcal{L}_{ttHH}^{\text{SMEFT}} = \frac{3(g_{\text{SM}} - ge^{i\xi})}{v} \frac{H^2}{2} t_L^\dagger t_R + \text{h.c.}}$$

$$W_L^- W_L^+ \to t\bar{t}H$$

$\sigma(W_L^- W_L^+ \to t\bar{t}H)$ (fb)

- SMEFT
- $(\sqrt{\hat{s}})^2/(100\text{TeV})^2 * \sigma_{100\text{TeV}}^\xi$
- $\xi = \pi$
- $\xi = 0.5\pi$
- $\xi = 0.25\pi$
- $\xi = 0.1\pi$

$\xi = 0$(SM)

$\sqrt{\hat{s}}$ (TeV)

above 10 TeV

$\sigma(W_L W_L \to t\bar{t}H)$ (fb)

- Complex Yukawa
- SMEFT*4
- $\xi = \pi$
- $\xi = 0.5\pi$
- $\xi = 0.25\pi$
- $\xi = 0.1\pi$

$\xi = 0$(SM)

$\sqrt{\hat{s}}$ (TeV)

$$\sigma_{\text{tot}}(W_L^- W_L^+ \to ttH)_{\text{SMEFT}} \approx \frac{1}{4}\sigma_{\text{tot}}(W_L^- W_L^+ \to ttH)_{\text{complex Yukawa}}$$

(a) **(b)**

Complete amplitude in SMEFT:

$$\mathcal{M}(W_L^- W_L^+ \to t\bar{t}H)_{\text{SMEFT}} = \sum_{k=1}^{20} \mathcal{M}_k + \mathcal{M}_{\text{Fig.}\mathbf{a}}$$

$$\mathcal{M}_{\text{Fig.}\mathbf{b}}^{\pm\pm} = \frac{1}{v^2}\left[\mp 2p_t\left(g_{\text{SM}} - g\cos\xi\right) - im_{tt}\left(g\sin\xi\right)\right]$$

$$\mathcal{M}_{\text{Fig.}\mathbf{a}}^{\pm\pm} = \frac{3}{v^2}\left[\mp 2p_t\left(g_{\text{SM}} - g\cos\xi\right) - im_{tt}\left(g\sin\xi\right)\right]\frac{(\hat{s} - 2m_W^2)}{(\hat{s} - m_H^2)}$$

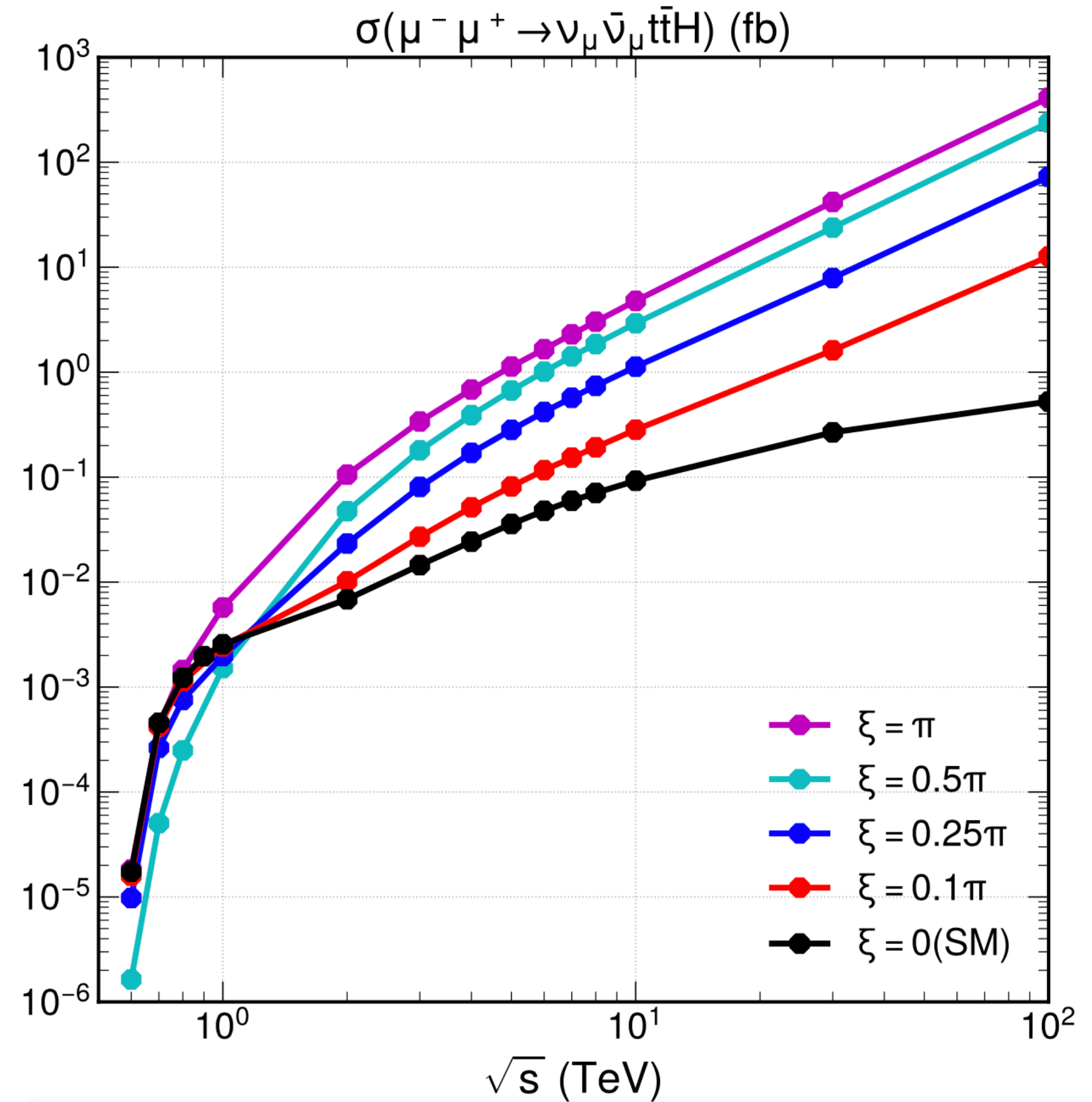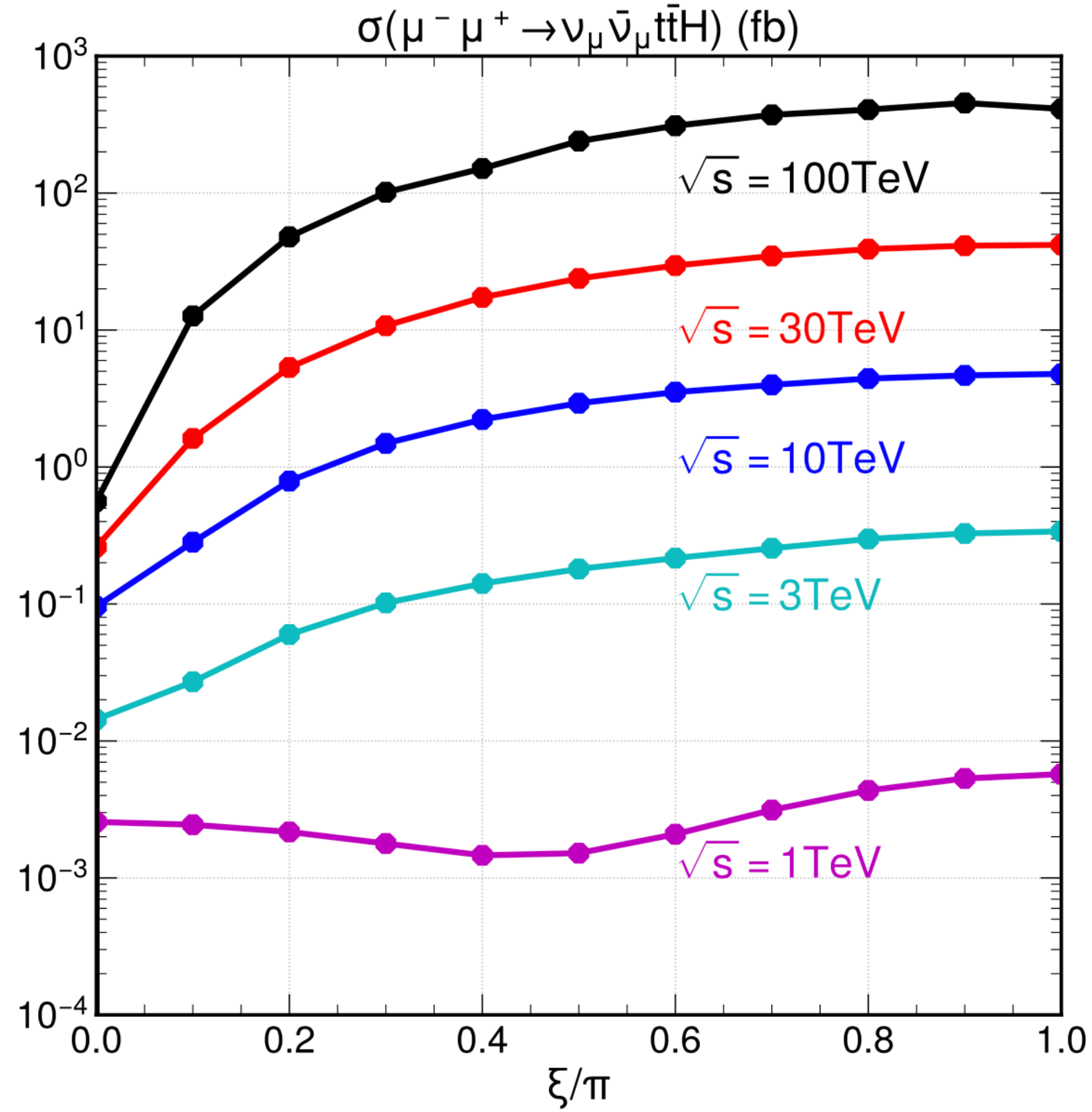$$\mathcal{M}_{\text{Fig.}\mathbf{a}}^{\pm\pm} = 3\mathcal{M}_{\text{Fig.}\mathbf{b}}^{\pm\pm} \cdot \left\{1 + \mathcal{O}\left(\frac{1}{\hat{s}}\right)\right\}$$

GBET tells:

$$\sum_{k=1}^{20} \mathcal{M}_k + \mathcal{M}_{\text{Fig.}\mathbf{a}} = \mathcal{M}_{\text{Fig.}\mathbf{b}} \cdot \left\{1 + \mathcal{O}\left(\frac{1}{\hat{s}}\right)\right\}$$

$$\sum_{k=1}^{20} \mathcal{M}_k \approx -2\mathcal{M}_{\text{Fig.}\mathbf{b}}$$

$\mu^-\mu^+ \rightarrow \nu_\mu \bar{\nu}_\mu t\bar{t}H$ in SMEFT

Phenomenologies under study, V. Barger, K. Hagiwara, J. Kanzaki, K.Mawatari and YJZ, in preparation

Perturbative Unitarity

In the SM, $g_{\rm SM} = m_t/v$, unitarity should be valid at all scales

When $\xi \neq 0$, perturbation unitarity can be violated at $\sqrt{s} \geq O\left(\dfrac{\Lambda}{\sqrt{\lambda}}\right)$ $\quad g_{\rm SM} - g e^{i\xi} = \dfrac{\lambda v^2}{\sqrt{2}\Lambda^2}$

Optical Theorem: $2 Im(T_{ii}) = \displaystyle\sum_f |T_{fi}|^2 \Phi_f = 2\hat{s} \sum_f \sigma(i \to f)$

$$SS^\dagger = 1$$

$$(1 + iT)(1 - iT^\dagger) = 1$$

$$-i(T - T^\dagger) = TT^\dagger$$

$$-i\langle i|(T - T^\dagger)|i\rangle = \langle i|TT^\dagger|i\rangle$$

$$-i(T_{ii} - T_{ii}^*) = \langle i|T|f\rangle \, \Phi_f \, \langle f|T^\dagger|i\rangle$$

All final states with phase space Φ_f

Unitarity bound:
for $J=0$
i=j

$$2Im(T_{ii}) > |T_{ii}|^2 \dfrac{1}{8\pi}$$ 2-body phase space

$$|T_{ii}|^2 < 16\pi \, Im(T_{ii}) < 16\pi |T_{ii}|$$

$$|T_{ii}| < 16\pi$$

$$2\hat{s} \sum_f \sigma(i \to f)_{J=0} = 2 Im(T_{ii})_{J=0} < 32\pi$$

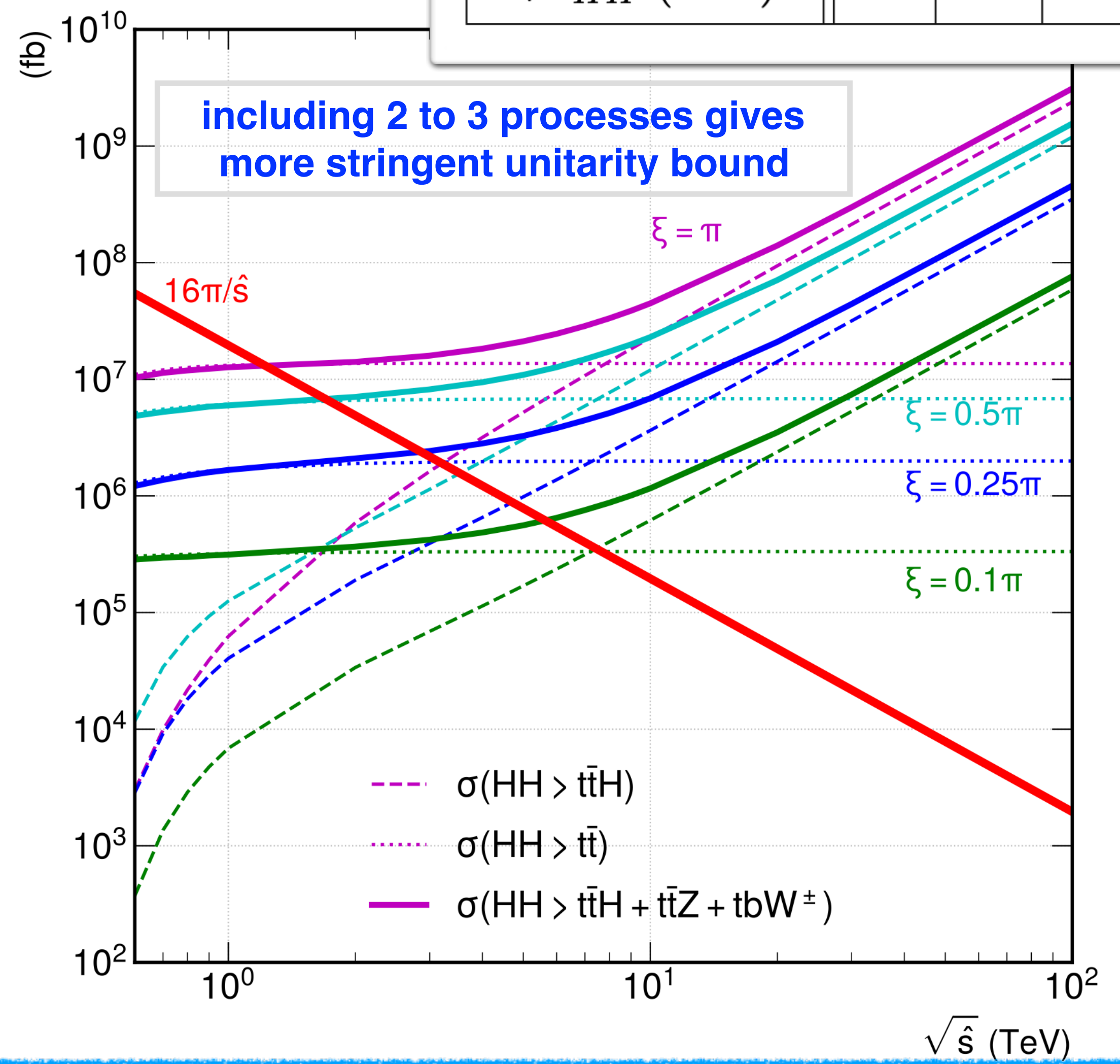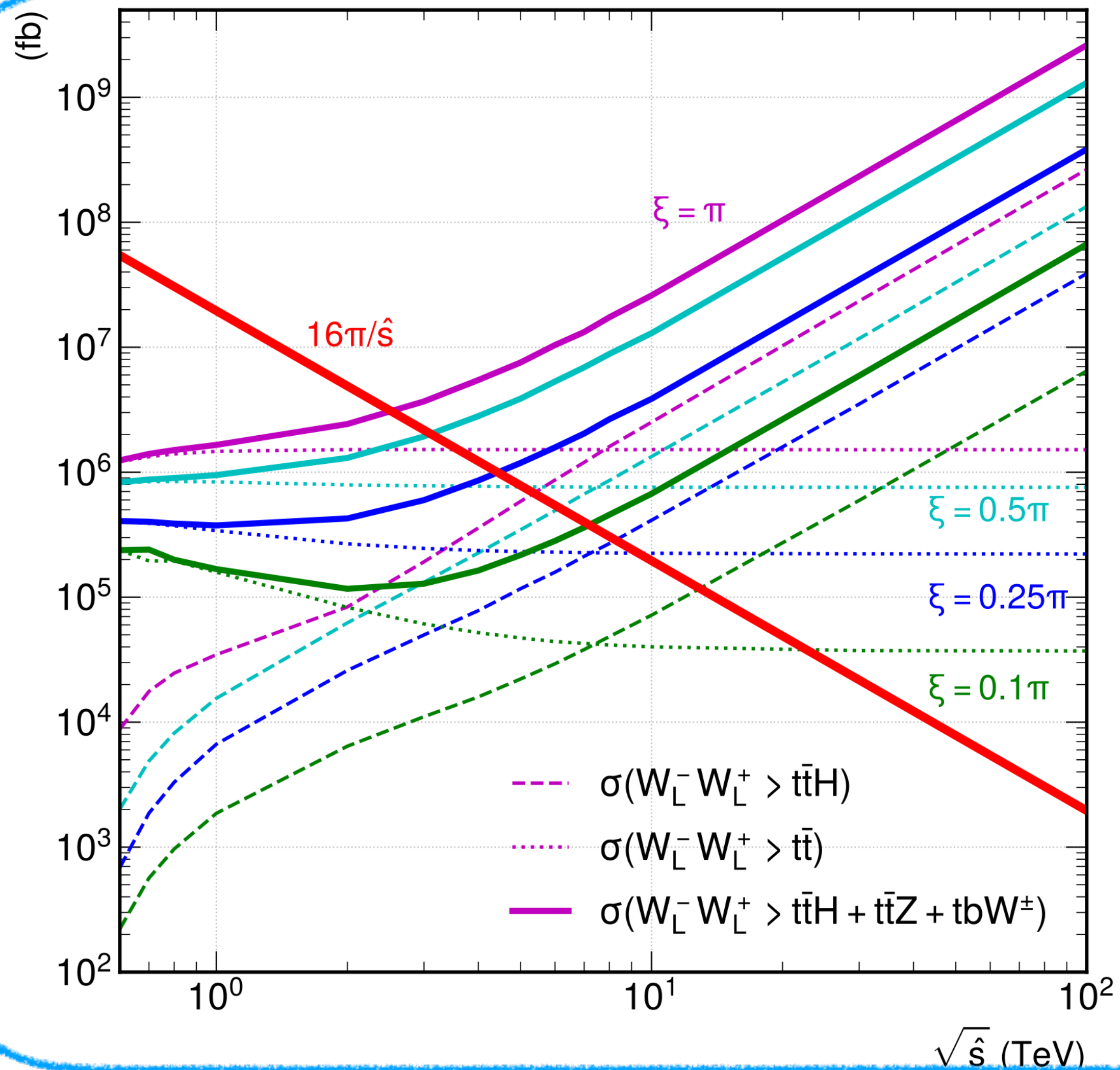$$\sum_f \sigma(i \to f)_{J=0} < \dfrac{16\pi}{\hat{s}}$$

Unitarity bound

$$\sum_f \sigma_{\text{tot}} \left(W_L^- W_L^+ \to f; J = 0 \right) < \frac{16\pi}{\hat{s}}$$

$$\sum_f \sigma_{tot} \left(HH \to f; J = 0 \right) < \frac{16\pi}{\hat{s}}$$

$|\xi|$	π	0.5π	0.25π	0.1π
$|\lambda| \cdot \Lambda^{-2}(\text{TeV}^{-2})$	32.9	23.2	12.6	5.14
$\sqrt{\hat{s}}_{W_L W_L}(\text{TeV})$	2.5	3.1	4.4	7.2
$\sqrt{\hat{s}}_{HH}$ (TeV)	1.2	1.7	2.9	5.6

including 2 to 3 processes gives more stringent unitarity bound

Feynman-Diagram (FD) gauge

- Weak bosons are 5-components $W^{\pm M} = (W^{\pm \mu}, \pi^{\pm})$, unlike in R_ξ gauge, EOM mixes $W^{\pm \mu}$ and $\pi^{\pm}$

- FD gauge propagator

$$G_{MN}(q) = \frac{i}{q^2 - m^2 + i\epsilon} \begin{pmatrix} -g_{\mu\nu} + \dfrac{q_\mu n_\nu + n_\mu q_\nu}{n \cdot q} & i\dfrac{m\, n_\mu}{n \cdot q} \\ -i\dfrac{m\, n_\nu}{n \cdot q} & 1 \end{pmatrix} \qquad n(q)^\mu_{\mathrm{FD}} = (\mathrm{sgn}(q^0), -\vec{q}/|\vec{q}|)$$

$$M, N = 0 \text{ to } 4,$$

- Helicity ±1 states don't mix with the Goldstone boson. Helicity 0 state is a mixture of

$$-\frac{Q\, n^\mu}{n \cdot q} = \epsilon^\mu(q, h = 0) - \frac{q^\mu}{Q}, \quad Q = \sqrt{|q^2|}$$

and the Goldstone boson.

- Because the Goldstone bosons are parts of the physical weak boson, all Goldstone boson vertices contribute to the scattering amplitudes in the FD gauge
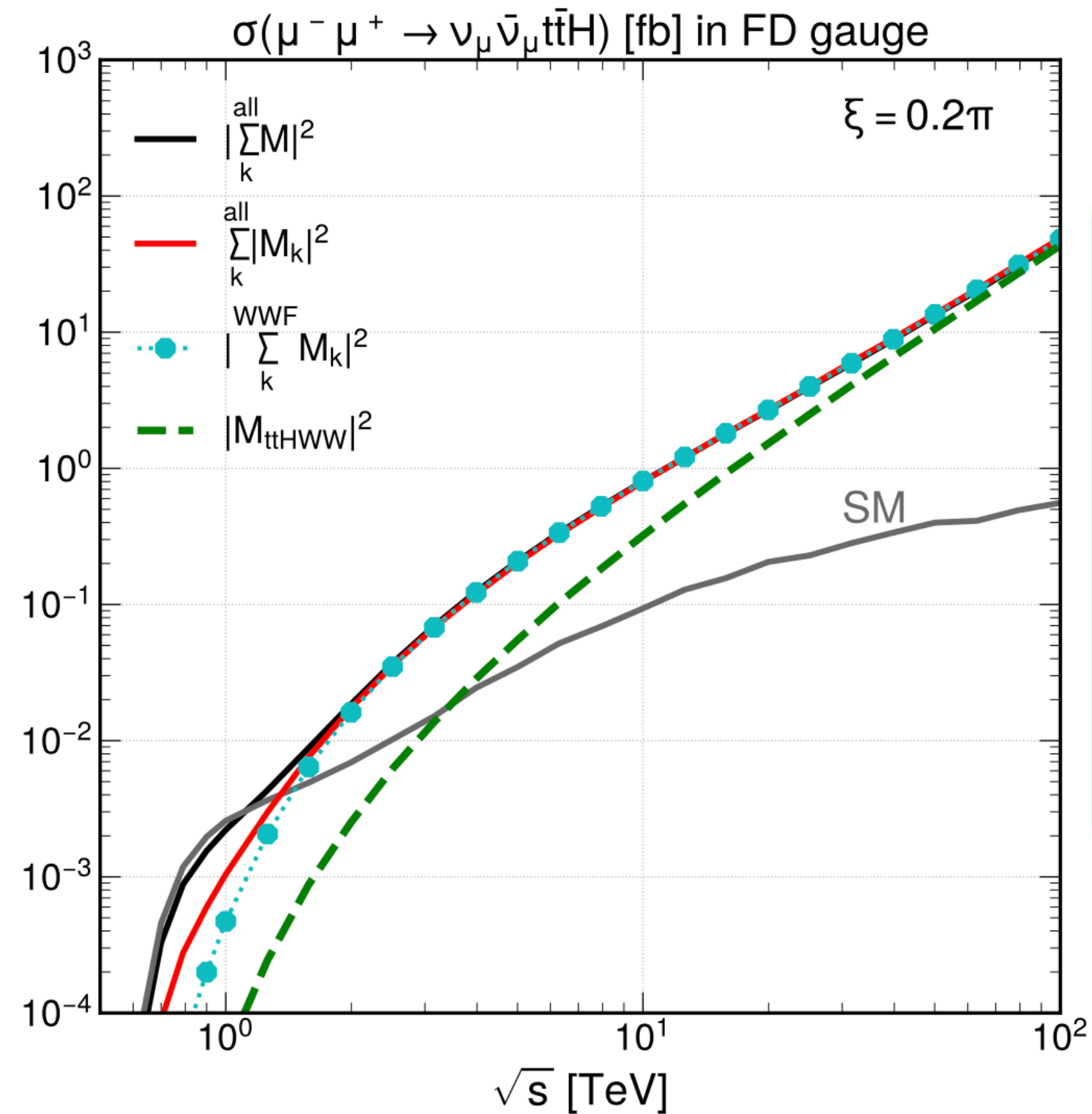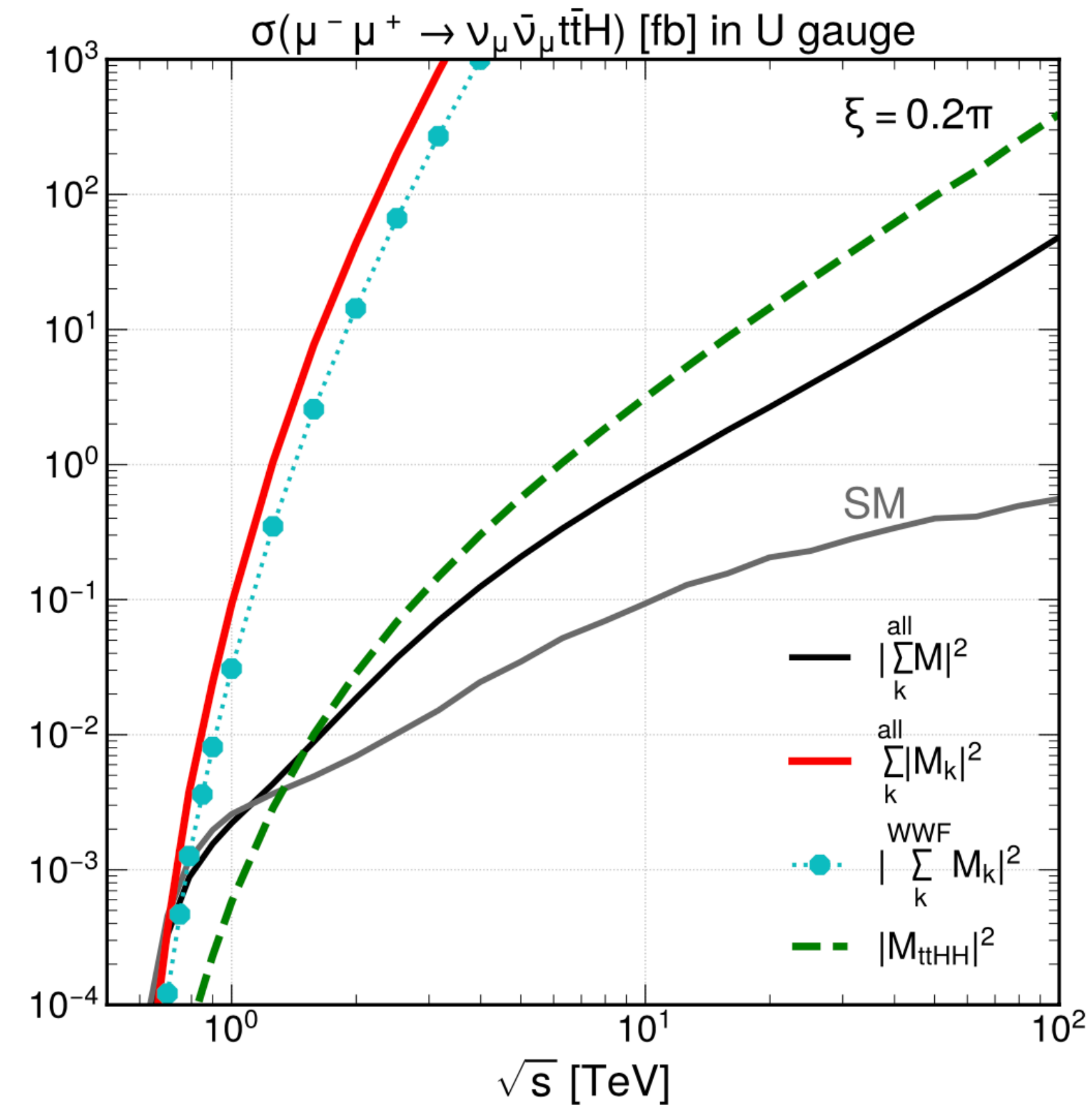
[1] Kaoru Hagiwara, Junichi Kanzaki and Kentarou Mawatari, 'QED and QCD helicity amplitudes in Parton-shower gauge.' Eur.Phys.J.C 80(2020) 6, 584
[2] Junmou Chen, Kaoru Hagiwara, Junichi Kanzaki and Kentarou Mawatari, 'Helicity amplitudes without gauge cancellation for electroweak processes'Eur.Phys.J.C 83 (2023).
[3] Junmou Chen, Kaoru Hagiwara, Junichi Kanzaki, Kentarou Mawatari and YJZ, 'Helicity amplitudes in light-cone and Feynman-diagram gauges'Eur.Phys.J.Plus 139 (2024).
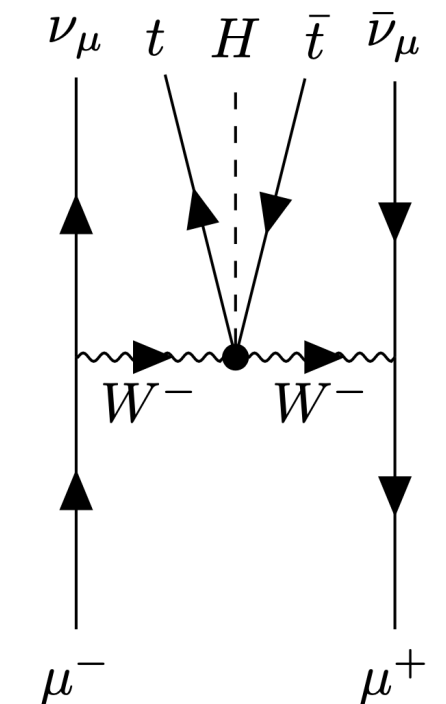
FD gauge

$\sigma(\mu^-\mu^+ \to \nu_\mu\bar{\nu}_\mu t\bar{t}H)$ [fb] in U gauge

$\xi = 0.2\pi$

Legend:
- black: $|\sum\limits_{k}^{all} M|^2$
- red: $\sum\limits_{k}^{all} |M_k|^2$
- cyan dotted: $|\sum\limits_{k}^{WWF} M_k|^2$
- green dashed: $|M_{ttHH}|^2$

SM

$\sigma(\mu^-\mu^+ \to \nu_\mu\bar{\nu}_\mu t\bar{t}H)$ [fb] in FD gauge

$\xi = 0.2\pi$

Legend:
- black: $|\sum\limits_{k}^{all} M|^2$
- red: $\sum\limits_{k}^{all} |M_k|^2$
- cyan dotted: $|\sum\limits_{k}^{WWF} M_k|^2$
- green dashed: $|M_{ttHWW}|^2$

SM

$\sqrt{s}$ [TeV]

- In this process, e.g.

$$\frac{g_{SM} - g e^{i\xi}}{v^2}\pi^+\pi^- H t_L^\dagger t_R + \text{h.c.}$$

contributes as

and dominates the total cross section because of its dim-6 property.

In the unitary gauge, the high energy dominance of VBF diagrams are understood from GBET but there are subtle gauge cancellation between VBF and other diagrams.

In the FD gauge, VBF-diagram dominance at high energy is manifest and specifically for the highest dimensional interaction, dim-6 ttHWW.

For arbitrary gauge models, automatic generation of FD gauge is available in Madgraph by command 'set gauge FD'.

Summary

- We identify the cause of a power law increase of the $\mu^-\mu^+ \to \nu\nu t t H$ cross section when the top Yukawa coupling is complex as due to the power law increase of the weak boson fusion sub process cross section, which is a consequence of gauge non-invariance of the dimension four Lagrangian.

- We identify the dimension-six SMEFT operator which gives a gauge invariant description for complex Yukawa coupling and confirm that the total cross section for $W W \to t t H$ satisfies the Goldstone Boson Equivalence Theorem.

- We obtain a novel perturbative unitarity bound on the SMEFT operator by summing over all $2 \to 2$ and $2 \to 3$ processes which contribute to the $J=0$ $HH \to HH$ amplitude.

- In the Feynman-Diagram gauge, the cross section is dominated by the WBF diagrams making the GBET manifest.